A NOVEL APPROACH OF FAST AND ADAPTIVE BIDIMENSIONAL EMPIRICAL MODE DECOMPOSITION

Sharif M. A. Bhuiyan[*], *Reza R. Adhami*, *Jesmin F. Khan*

Department of Electrical and Computer Engineering, University of Alabama in Huntsville
Huntsville, Alabama 35899, USA, [*]Email: bhuiyas@ece.uah.edu

ABSTRACT

Bidimensional empirical mode decomposition (BEMD) techniques are associated with high computation time and other artifacts because of the application of two dimensional (2D) scattered data interpolation methods. In this paper, order statistics filters are employed to get the upper and lower envelopes in the BEMD process, instead of the surface interpolation. Based on the achieved characteristics of the proposed approach, it is considered as fast and adaptive BEMD (FABEMD). Simulation results demonstrate that besides reducing the computation time, FABEMD outperforms the original BEMD in terms of the quality in some cases.

Index Terms– Bidimensional empirical mode decomposition (BEMD), envelope estimation, order-statistics filter.

1. INTRODUCTION

Empirical mode decomposition (EMD) is a relatively new concept in the area of signal processing [1]. The complete process of decomposing a signal into its intrinsic mode functions (IMFs) and finding the time frequency distribution is also known as the Hilbert-Huang transform (HHT) [1]. The technique extended to analyze two-dimensional (2D) data is known as bidimensional EMD (BEMD) and/or 2D EMD [2-5]. Like EMD, BEMD require finding local maxima and minima points (jointly known as local extrema points) and subsequent interpolation of those points.

Extraction of each IMF requires several iterations. Because the surface interpolation method itself fits a surface in an iterative optimization approach, it makes the BEMD process complex and excessively time consuming. Effects of incorrect interpolation due to the lack of extrema points at the boundary region and very few arbitrarily distributed extrema points at some stages of the process impose severe restriction on the application of BEMD. Although a few modifications have been suggested in the literature to improve the process [4-8], BEMD still suffers from the above mentioned problems to some extent.

In this paper, a novel BEMD approach is proposed, which replaces the interpolation step by a direct envelope estimation method. In this technique, spatial domain sliding order-statistics filters, namely *MAX* and *MIN* filters, are employed to get the running maxima and minima of the data. Application of smoothing operation to the running maxima and minima results in the desired upper and lower envelopes, respectively. The size of the order-statistics filters is derived from the available information of maxima and minima maps. Since the proposed BEMD process results in faster computation and incorporates adaptability, this process has been named as fast and adaptive BEMD (FABEMD). Although complete HHT analysis is possible with BEMD or FABEMD, the decomposition of an image into BIMFs alone offers a wide variety of image processing applications.

2. BEMD OVERVIEW

BEMD decomposes an image into its bidimensional IMFs (BIMFs) and a Residue based on the local spatial scales [2-4]. The BIMFs are expected to have the following properties [2, 3]: (i) at any point, the mean value of the upper and lower envelopes, defined by the local maxima and minima points, is zero; and (ii) they are locally orthogonal to each other.

Let the original image be denoted as I, a BIMF as F, and the Residue as R. In the process, i-th BIMF F_i is obtained from its source image S_i, where $S_i=S_{i-1}-F_{i-1}$ and $S_1=I$. It requires one or more iterations to obtain F_i, where the intermediate state of a BIMF (IS-BIMF) in j-th iteration can be denoted as F_{Tj}. The steps of the BEMD process can be summarized as below [1-3].

i) Set $i = 1$ and $S_i = I$.
ii) Set $j = 1$ and $F_{Tj}=S_i$.
iii) Obtain the local maxima map of F_{Tj}, denoted as P_j; and local minima map of F_{Tj}, denoted as Q_j.
iv) Generate the upper envelope (UE) U_{Ej} and the lower envelope (LE) L_{Ej} of F_{Tj}, by interpolating the maxima points in P_j and the minima points in Q_j, respectively.
v) Find the mean envelope (ME) as $M_{Ej}=(U_{Ej}+L_{Ej})/2$.
vi) Calculate F_{Tj+1} as $F_{Tj+1}=F_{Tj}-M_{Ej}$.
vii) Check whether F_{Tj+1} follows the BIMF properties by finding the standard deviation (SD), denoted as D, between F_{Tj+1} and F_{Tj} defined below and comparing it to the desired threshold.

$$D=\frac{\sum_{x=1}^{M}\sum_{y=1}^{N}\left|F_{Tj+1}(x,y)-F_{Tj}(x,y)\right|^2}{\sum_{x=1}^{M}\sum_{y=1}^{N}\left|F_{Tj}(x,y)\right|^2}, \quad (1)$$

where (x,y) is the coordinate, M is the total number of rows and N is the total number of columns of the 2D data.
viii) If F_{Tj+1} meets the criteria as per step (vii), then take $F_i=F_{Tj+1}$; set $S_{i+1}=S_i$ and $i=i+1$; go to step (ix). Otherwise set $j=j+1$, go to step (iii) and continue up to step (viii).
ix) Determine if S_i has less than three extrema points, and if so, the Residue, $R=S_i$; and the decomposition is complete. Otherwise, go to step (ii) and continue up to step (ix).

Let the BIMFs and the Residue of an image together be named as bidimensional empirical mode components (BEMCs). An orthogonality index (OI), denoted as O, may be defined for the BEMCs as below following Ref. [1].

$$O=\sum_{x=1}^{M}\sum_{y=1}^{N}\left(\sum_{i=1}^{K+1}\sum_{j=1}^{K+1}\frac{C_i(x,y)C_j(x,y)}{{\Sigma_C}^2(x,y)}\right), \quad (2)$$

where, C_i is the i-th BEMC, K is the total number of BIMFs and Σ_C is the summation of the BEMCs. A low value of OI indicates a good decomposition in terms of local orthogonality.

3. FABEMD ALGORITHM DETAILS

FABEMD differs from the original BEMD algorithm, basically in the process of estimating the upper and lower envelopes and in limiting the number of iterations per BIMF to one. Hence the steps of the FABEMD algorithm are the same as original BEMD given in Section 2 with maximum required value of j equal to one considered being sufficient.

Like BEMD, neighboring window method [2] is employed to find the local maxima and minima points. In this method a data point is considered as a local maximum (minimum), if its value is strictly higher (lower) than all of its neighbors within a window. Generally, a 3×3 window results in optimum extrema maps for a given 2D data.

After obtaining the maxima and minima maps, P_j and Q_j, respectively, from a given F_{Tj}, it is required to create the continuous upper and lower envelopes, U_{Ej} and L_{Ej}. In usual BEMD, suitable 2D scattered data interpolation is applied to P_j and Q_j to create these envelopes. In this work a simple but efficient method has been formulated for this purpose. This approach applies two order statistics filters to approximate the envelopes, where a *MAX* filter is used for the upper envelope and a *MIN* filter is used for the lower envelope. The size of these filters are determined based on the maxima and minima maps obtained from corresponding source image S_i, i.e. based on P_j and Q_j derived from F_{Tj} when j=1 and F_{Tj}=S_i. For each local maximum (minimum) point in P_j (Q_j), the Euclidean distance to the nearest other local maximum (minimum) point is calculated and stored in an array, denoted as $\mathbf{d}_{\mathbf{adj\text{-}max}}$ ($\mathbf{d}_{\mathbf{adj\text{-}min}}$), where the number of elements is equal to the number of local maxima (minima) points in the maxima (minima) map P_j (Q_j). Considering square window, the gross window width $w_{en\text{-}g}$ for order statistics filters can be selected in different ways using the distance values in $\mathbf{d}_{\mathbf{adj\text{-}max}}$ and $\mathbf{d}_{\mathbf{adj\text{-}min}}$ among which two choices are considered here as given below.

$$w_{en\text{-}g} = \min\{\min\{\mathbf{d}_{\mathbf{adj\text{-}max}}\}, \min\{\mathbf{d}_{\mathbf{adj\text{-}min}}\}\} \quad (3)$$

$$w_{en\text{-}g} = \max\{\max\{\mathbf{d}_{\mathbf{adj\text{-}max}}\}, \max\{\mathbf{d}_{\mathbf{adj\text{-}min}}\}\} \quad (4)$$

where, max{} denotes the maximum value of the elements in the array {} and min{} denotes the minimum value of the elements in the array {}. $w_{en\text{-}g}$ is rounded to the nearest odd integer to get the final window width w_{en}. Let the order statistics filter widths (OSFWs) obtained via Eqs. (3) and (4) be defined as lowest distance (LD) and highest distance (HD), respectively. w_{en} required for i+1-th BIMF generally appears larger than that for i-th BIMF if using HD OSFW; however, w_{en} for i+1-th BIMF sometimes may not appear larger than that for i-th BIMF if using LD OSFW. Therefore, if the calculated w_{en} for a BIMF mode is not larger than the previous BIMF mode, then additional manipulation may be done to make it larger than the previous mode. It will ensure the existing properties of BIMF hierarchy in the sense that the later BIMF will contain coarser local spatial scales [1,2]. On the other hand, w_{en} may be chosen arbitrarily as well. In that case, w_{en} for i+1-th BIMF should be chosen higher than the w_{en} for i-th BIMF; but extraction of BIMFs will be less data driven with an arbitrary selection of w_{en}. The various possibilities of window sizes for *MAX* and *MIN* filters provide different decomposition of an image. This feature of variable window size selection makes the proposed approach an adaptive one. The choice of w_{en} from the various options depends on the application and/or desired BIMF characteristics.

With the determination of window size w_{en}, *MAX* and *MIN* filters are applied to the corresponding IS-BIMF F_{Tj} to obtain the upper and lower envelopes, U_{Ej} and L_{Ej}, as specified below.

$$U_{Ej}(x,y) = \underset{(s,t)\in Z_{xy}}{MAX}\left\{F_{Tj}(s,t)\right\}, \quad (5)$$

$$L_{Ej}(x,y) = \underset{(s,t)\in Z_{xy}}{MIN}\left\{F_{Tj}(s,t)\right\}. \quad (6)$$

In Eq. (5) the value of the upper envelope U_{Ej} at any point (x,y) is simply the maximum value of the elements in F_{Tj} in the region defined by Z_{xy}, where Z_{xy} is the square region of size w_{en}×w_{en} centered at any point (x,y) of F_{Tj}. Similarly, in Eq. (6) the value of the lower envelope L_{Ej} at any point (x,y) is simply the minimum value of the elements in F_{Tj} in the region defined by Z_{xy}. To obtain smooth continuous surfaces for upper and lower envelopes, averaging smoothing operations are carried out on both U_{Ej} and L_{Ej}, which may be expressed as below.

$$U_{Ej}(x,y) = \frac{1}{w_{sm}\times w_{sm}} \sum_{(s,t)\in Z_{xy}} U_{Ej}(s,t) \quad (7)$$

$$L_{Ej}(x,y) = \frac{1}{w_{sm}\times w_{sm}} \sum_{(s,t)\in Z_{xy}} L_{Ej}(s,t), \quad (8)$$

where Z_{xy} is the square region of size w_{sm}×w_{sm} centered at any point (x,y) of U_{Ej} or L_{Ej}, w_{sm} is the window width of the averaging smoothing filter and w_{sm}=w_{en}. From the smoothed envelopes, U_{Ej} and L_{Ej}, the mean or average envelope M_{Ej} is calculated as in the original BEMD method given in Section 2.

To illustrate the envelope formation for FABEMD, let us consider a 1D signal for simplicity, given in Fig. 1. The local maxima and minima points for this signal are obtained using a 1×3 neighboring window, which gives $\mathbf{d}_{\mathbf{adj\text{-}max}}$=[107 106 93 93 72] and $\mathbf{d}_{\mathbf{adj\text{-}min}}$=[108 107 93 93 78]. Using these distance arrays, LD and HD OSFWs appear to be 73 and 109, respectively. Taking HD OSFW (w_{en}=w_{sm}=109) as the width of the *MAX* or *MIN* filter and applying them to the maxima and minima maps results in the UE, LE and ME shown in Fig. 1(a). The corresponding envelopes after applying averaging smoothing filter are displayed in Fig. 1(b), and the same envelopes created by applying cubic spline interpolation (CSI) [1] to the maxima and minima maps are given in Fig. 1(c). The top waveforms in Figs. 2(a) and 2(b) are the original 1D signal given in Fig. 1, whereas the bottom waveform in Fig 2(a) is the result of ME subtraction in FABEMD method and the bottom waveform in Fig. 2(b) is the result of ME subtraction in BEMD method. This illustration demonstrates that the proposed approach of envelope estimation in FABEMD can be a suitable alternative to regular envelope estimation using interpolation in BEMD.

4. SIMULATION RESULTS

FABEMD results are reported for both LD and HD OSFWs and for one and more than one iterations. On the other hand, BEMD results are shown for thin-plate spline (TPS) interpolation, which is a good choice for BEMD [3-5]. SD criterion is employed as the fundamental stopping criteria with a threshold of 0.01 while the maximum number of allowable iterations (MNAI) is applied as an additional stopping criterion for BEMD. In the simulation, the maximum image size is limited to 256×256-pixel. Although FABEMD is capable of decomposing images of any size or resolution very fast, BEMD is unable to do so. Since FABEMD results are compared with BEMD results for the same images, 256×256-pixel images help perform the task conveniently.

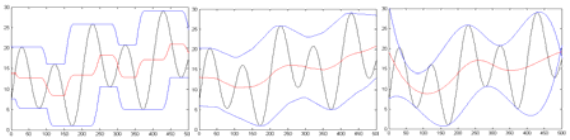

(a) (b) (c)

Fig. 1. A 1D signal and its envelopes using (a) FABEMD before smoothing, (b) FABEMD after smoothing, (c) BEMD with CSI.

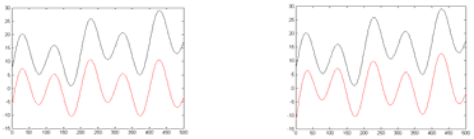

(a) (b)

Fig. 2. (a) Original signal (top) and mean envelope subtracted signal using FABEMD algorithm, (b) Original signal (top) and mean envelope subtracted signal using BEMD algorithm.

A synthetic texture image (STI) shown in Fig. 3(d) is considered first, which is derived from the addition of three components (STCs) given in Figs. 3(a), 3(b) and 3(c). The BEMCs of the STI obtained by applying FABEMD with HD-OSFW are displayed in Fig. 4 for MNAI=1 and in Fig. 5 for MNAI=5. Similarly, the BEMCs of the STI obtained by applying BEMD with RBF-TPS are displayed in Fig. 6 for MNAI=1 and in Fig. 7 for MNAI=5. Table 1 displays the number of obtained BEMCs, time taken and OI; while Table 2 shows the stopping point SD for each BIMF for each method considered. From the visual and quantitative evaluation, FABEMD with HD-OSFW for MNAI=1 appears to be a good choice for decomposition of the STI in Fig. 3(d).

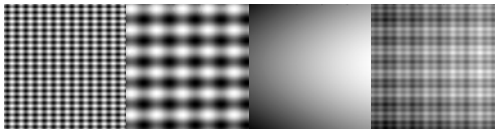

(a) (b) (c) (d)

Fig. 3. (a) STC-1, (b) (STC-2, (c) STC-3, (d) Original synthetic texture image (STI) obtained from addition of (a) to (c).

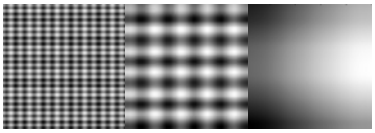

Fig. 4. BEMCs of the STI obtained by FABEMD with HD OSFW (MNAI=1).

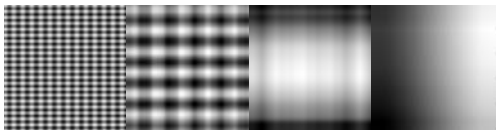

Fig. 5. BEMCs of the STI obtained by FABEMD with HD OSFW (MNAI=5).

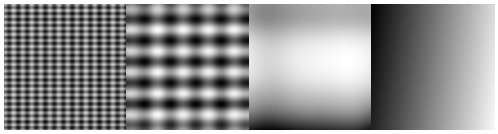

Fig. 6. BEMCs of the STI obtained by BEMD with RBF-TPS (MNAI=1).

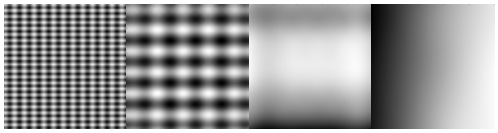

Fig. 7. BEMCs of the STI obtained by BEMD with RBF-TPS (MNAI=5).

Table 1. Comparison among various BEMD approach for the STI in terms of total number of BEMCs, total time required and OI.

	FABEMD		BEMD	
	HD-OSFW MNAI=1	HD-OSFW MNAI=5	RBF-TPS MNAI=1 D=0.01	RBF-TPS MNAI=5 D=0.01
Total BEMC	3	4	4	4
Time (Sec)	14.6986	446.6392	205.5114	975.3234
OI	0.0342	0.0581	0.0988	0.664

Table 2. Comparison among various BEMD approach for the STI in terms of achieved stopping point SD for each BIMF.

	FABEMD		BEMD	
	HD-OSFW MNAI=1	HD-OSFW MNAI=5	RBF-TPS MNAI=1 D=0.01	RBF-TPS MNAI=5 D=0.01
BIMF-1	0.98159	0.02355	0.98337	0.00673
BIMF-2	0.99306	0.02875	0.99189	0.01256
BIMF-3	-	0.03691	0.90914	0.01664

Two real images are considered next, which are a 256×256-pixel region of a real texture image, D18, taken from the Brodatz texture set and shown in Fig. 8(a) [9]; and a sub-sampled 256×256-pixel Elaine image shown in Fig. 8(b). The BEMCs generated from the D18 image and Elaine image by applying FABEMD with LD-OSFW and MNAI=1 are shown in Figs. 9 and 11, respectively. On the other hand, the BEMCs generated from these same images by applying BEMD with RBF-TPS interpolation and MNAI=10 are shown in Figs. 10 and 12, respectively. It is obvious from the simple visual evaluation of the BEMCs of real images that FABEMD yields very well defined BEMCs that represent the image features at various spatial scales similar to or better than the BEMCs obtained from the BEMD method.

(a) (b)

Fig. 8. (a) A 256×256-pixel region of Brodatz texture D18 [9], (b) 256×256-pixel Elaine image.

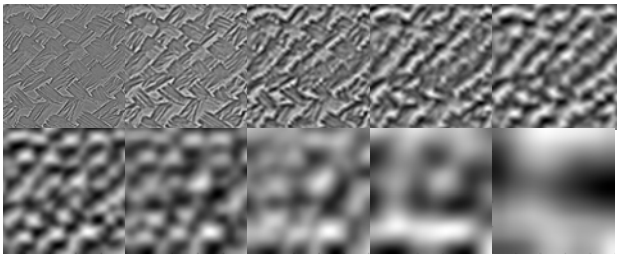

Fig. 9. BEMCs of D18 image obtained by FABEMD with LD-OSFW (MNAI=1).

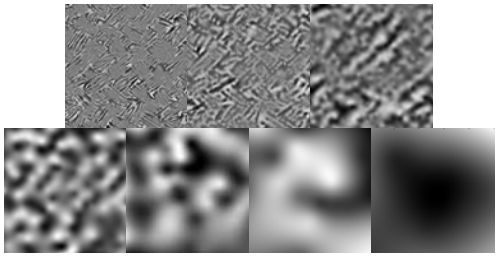

Fig. 10. BEMCs of D18 image obtained by BEMD with RBF-TPS (MNAI=10).

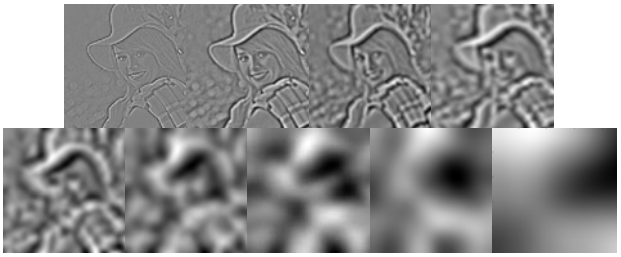

Fig. 11. BEMCs of Elaine image obtained by FABEMD with LD-OSFW (MNAI=1).

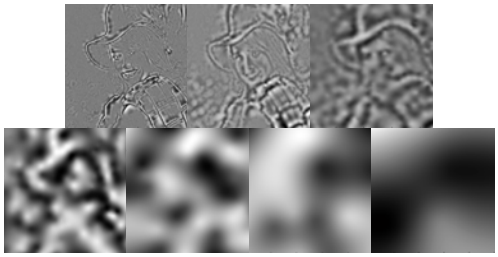

Fig. 12. BEMCs of Elaine image obtained by BEMD with RBF-TPS (MNAI=10).

Unwanted distortion and other artifacts may accompany the BEMCs when obtained via BEMD, which is apparent from the above figures of BEMCs. Envelope estimation in FABEMD, employing order-statistics filters, is nearly independent of the image or texture pattern in terms of complexity and processing time; and the envelopes closely follow the image. But, envelope estimation in the BEMD method, employing surface interpolation, is highly dependent on the maxima or minima maps while the envelopes are not guaranteed to follow the image. For real images, the time taken by BEMD is extremely higher than that required by FABEMD. While FABEMD takes only a few minutes, BEMD takes many hours, even for a very few iterations performed per BIMF. This problem hinders the application of BEMD in many practical cases.

5. CONCLUSION

To enhance BEMD for image processing applications, a fast, time efficient and effective method is essential. This fact motivated the formulation of the proposed fast and adaptive BEMD, abbreviated as FABEMD. In FABEMD, the envelope estimation method of regular BEMD is modified by replacing the 2D surface interpolation by an order-statistics based filtering followed by a smoothing operation. A number of window sizes can be selected for the order-statistics and smoothing filters, all of which are data driven and thus making the process adaptive. The simple change in the envelope estimation procedure provides a tremendous enhancement of the algorithm in terms of computation time. Simulation results demonstrate the usefulness of this novel FABEMD approach for BEMD based image decomposition. Besides reducing the computation time, this novel approach also ensures a more accurate estimation of the BIMFs in some cases.

6. REFERENCES

[1] N. E. Huang, et al., "The empirical mode decomposition and the Hilbert spectrum for non-linear and non-stationary time series analysis," *Proc. of Royal Society of London A*, Vol. 454, pp. 903–995, 1998.

[2] J. C. Nunes, Y. Bouaoune, E. Delechelle, O. Niang, Ph. Bunel, "Image analysis by bidimensional empirical mode decomposition," *Image and Vision Computing*, Vol. 21 pp. 1019–1026, 2003.

[3] A. Linderhed, "2D empirical mode decompositions - in the spirit of image compression," *Proc. of SPIE*, Vol. 4738, pp. 1-8, 2002.

[4] C. Damerval, S. Meignen, V. Perrier, **"**A fast algorithm for bidimensional EMD," *IEEE Signal Processing Letters*, Vol. 12, No. 10, pp. 701-704, 2005.

[5] Z. Liu, H. Wang, S. Peng, "Texture classification through directional empirical mode decomposition," *Proc. of the 17th International Conference on Pattern Recognition – ICRP 2004*, pp. 803-806, Cambridge UK, August 2004.

[6] Zhongxuan Liu, and Silong Peng, "Boundary Processing of Bidimensional EMD Using Texture Synthesis," *IEEE Signal Processing Letters*, Vol. 12, No. 1, pp. 33-36, 2005.

[7] Z. Liu, "A novel boundary extension approach for empirical mode decomposition," *Proceedings of International Conference on Intelligent Computing* (ICIC 2006), (Eds.) D. Huang, K. Li, G. W. Irwin, pp. 299-304, Kunming, China, August 16-19, 2006.

[8] B. Huan, Q. Xie, S. Peng, "EMD sifting based on bandwidth," *IEEE Signal Processing Letters*, Vol. 14, No. 8, pp. 537-540, 2007.

[9] P. Brodatz, *Textures – A Photographic Album for Artists and Designers*, New York: Dover, 1966.